

# Spatial Dynamics and Risk Mapping of Forest Fires in Madhesh Province, Nepal: A Multi-Criteria Decision Approach

Gunjan Adhikari<sup>1</sup>, Khagendra Prasad Joshi<sup>2</sup>, Dristee Chad<sup>1</sup>, Ashish Ghimire<sup>1</sup>, and Sandeep Mahara<sup>1\*</sup>

<sup>1</sup>*Institute of Forestry, Pokhara Campus, Tribhuvan University, Pokhara, Nepal*

<sup>2</sup>*Central Department of Hydrology and Meteorology, Tribhuvan University, Nepal*

## ARTICLE INFO

Received: 30Apr 2024

Received in revised: 22 Nov 2024

Accepted: 2 Dec 2024

Published online: 6 Jan 2025

DOI: 10.32526/ennrj/23/20240124

### Keywords:

AHP/ Forest fire/ GIS/ MODIS

### \* Corresponding author:

E-mail: maharas450@gmail.com

## ABSTRACT

Forest fires in Nepal are a pressing environmental concern, impacting ecosystems and community livelihoods. This research aims to understand forest fires, their trends, distribution, and relation with selected variables found in the sub-tropical forests of Madhesh Province of Nepal, and then identify potential fire risks and vulnerable areas. The selected fire incidents were analyzed using fire points produced by the moderate resolution imaging spectroradiometer (MODIS) sensor. Following the analytic hierarchy process (AHP) approach, this research investigates topographic, climatic, biophysical, and anthropogenic variables to create a fire risk map. Throughout the 22-year research period (2001-2023), 6,368 fire incidents and 6,158.22 km<sup>2</sup> of total burnt area were reported in the study area. Overall, the Mann-Kendall test showed an increasing trend for regional fire incidents. It has been found that about 24% of the province is either at high or very high risk for fire. The validity of the prediction map was confirmed with an AUC value of 0.798. The findings of the study will be valuable to local, state, and federal governments, policymakers, forest fire managers, researchers, and land planners in building a landscape-level forest fire management plan for high-risk areas.

## 1. INTRODUCTION

Wildfire or forest fire, although an important component of biome development in forest ecosystem (Dawson et al., 2001; Doerr and Santín, 2016) has been a driving factor for forest degradation globally, and a major risk to Nepal's forest cover (Singh, 2017). Recurrent forest fires destroy non-timber forest products, severely harming and hindering seedling regeneration and growth, and, in some situations, facilitating the spread of exotic species (MoFSC, 2016).

Monitoring and assessment of forest fires and prone areas with remote sensing has been an effective approach for evaluating, regulating, and predicting fire risks (Qadir et al., 2021). Numerous geosynchronous satellites, including the along track scanning radiometer (ATSR) onboard, ERS-1 and 2 (European Remote Sensing Satellite 1 and 2), the moderate

resolution imaging spectroradiometer (MODIS) onboard the Terra and Aqua Satellites have been frequently used in monitoring forest fires (Curkovic, 2012). MODIS, acquiring its synoptic source of information from routine satellite observation on various temporal scales, has proven to be advantageous for the monitoring of forest fires (Reeves et al., 2006). In line with this, Pradhan et al. (2007) produced a susceptibility map based on the correlation between MODIS fire incident points and the associated contributing factors.

Among many techniques for calculating and modeling fire risk areas, multi-criterion decision analysis (MCDA) and geographic information system (GIS) have been most adopted (Wang et al., 1990; Joerin et al., 2001; Yu et al., 2011; Zolekar and Bhagat, 2018), where MCDA techniques offer solutions with user-defined needs. Different literatures

**Citation:** Adhikari G, Joshi KP, Chad D, Ghimire A, Mahara S. Spatial dynamics and risk mapping of forest fires in Madhesh Province, Nepal: A multi-criteria decision approach. Environ. Nat. Resour. J. 2025;23(1):80-94. (<https://doi.org/10.32526/ennrj/23/20240124>)

have prompted the use of MCDA techniques including analytical hierarchy process (AHP), Fuzzy AHP, and ANP (citations of papers using AHP, Fuzzy AHP, and ANP). Among others, AHP is a thorough structured technique for multi-criteria decision analysis (Kumar and Garg, 2017). Most importantly, integrating GIS and remote sensing with AHP approaches can give policymakers, social networks, forest fire managers, and other stakeholders credible information on when and where fires are predicted to occur.

Despite being a small nation with an area of 147,516 km<sup>2</sup>, 44.74% of Nepal's total land area is covered with forests and woodlands (FAO, 2020). Recent years have shown a growing trend of forest fires, where 2021 hit the worst-case scenario as compared to past trends (Parajuli et al., 2020). Madhesh Province represents the Terai region of Nepal and is second to the Chure range in terms of fire hotspots in Nepal (Ranabhat et al., 2022), however, no research work has addressed the recurrent wildfire patterns of the province. Thus, this study responds to the necessity of accurately mapping the wildfire risk zones to abate the possible abrasion of forest fires in the province. Such mapping of forest fire risk zones would eventually benefit Nepal's disaster preparedness measures (Parajuli et al., 2020). The current study considers the province for the most

recent trends in forest fires way forwarding further opportunities for filling the research void in forest fire dynamics of the province. This research identifies where and when the fires are most likely to occur in the study area, providing a crucial foundation for improving current forest fire control strategies.

## 2. METHODOLOGY

### 2.1 Study area

Madhesh province occupies the southern part of Nepal within an elevation range of 1,000-3,300 feet, located between 22.9734°N and 78.6569°E, and bordered by the Siwalik hills on the north, India in the south, the Koshi River in the east, and Bagmati Pradesh in the west. The province's lower tropical climate dominates over 90% of its total geographical area, with the remaining portion experiencing the upper tropical climate. Approximately 27.29% of the total land area is covered by forest in the province (DFRS, 2015). The major forest cover is occupied by *Shorea robusta* forest, followed by the forests of *Terminalia* and *Anogeissus*, *Dalbergia sissoo*-*Acacia catechu*, and *Bombax* riverine. The study primarily focuses on the forest region of the area as shown in Figure 1. Simultaneously Figure 2 provides the overall framework of methodological steps involved in this study.

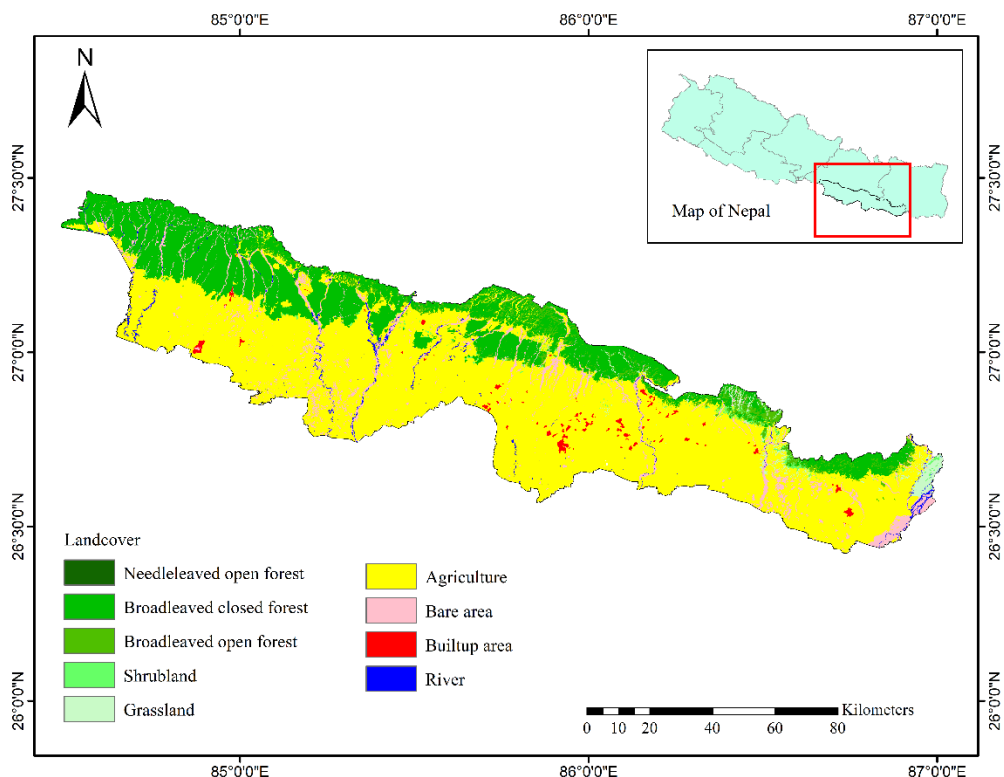


**Figure 1.** Landcover map of the study area (Source: ICIMOD, 2013)

## 2.2 Acquisition of dataset

Data available on active fires were extracted using the MODIS. The MODIS active fire product detects fires burning in  $1 \times 1 \text{ km}^2$  pixels under cloud-free conditions (Giglio et al., 2015; Giglio et al 2006). The fire incidences from 2001 to 2023 were obtained from [https://firms.modaps.eosdis.nasa.gov/active\\_fire/](https://firms.modaps.eosdis.nasa.gov/active_fire/) which provides the data for spatial-temporal analysis (Qadir et al., 2021). In MODIS, there are different levels of confidence from 0 to 100 in the detection intervals showing the accuracy of the data. We used the data exceeding 30% confidence level in this study to avoid false incidents but not ignore small fires before previous studies (Giglio et al., 2015; Parajuli et al., 2020).

In the current study, satellite data as well as other vector and raster data products were utilized. The parameters were divided into topographical (elevation, aspect, and slope), climatic (temperature), anthropogenic (distance from road and closeness to settlement), and biophysical categories (land cover). For the topographical data, Aster global DEM model V003 was downloaded from the USGS website (<https://earthexplorer.usgs.gov/>) (LP DAAC, 2019) and the area of interest was then mosaiced, projected,

and then clipped consecutively. Then, using the slope and aspect function in the ArcGIS 10.8 spatial analyst tool (ESRI, 2022), the slope and aspect were obtained from the DEM map. The data for land surface temperature was obtained by compiling MODIS data (MOD11C3) (Wan, 2014). The ArcGIS cell statistics tool was used to assemble and integrate the monthly data. For effectiveness, a distinct layer was created by averaging the mean monthly temperature for each year's pre-monsoon season (March-May) since the majority of forest fire cases occur in this season (Matin et al., 2017; Parajuli et al., 2020). Similarly, landcover data for the year 2010 was obtained from (ICIMOD, 2013) providing the classification of all the forest types. The data from this year was used since no other open-source layers provided the classification of the forest types. The dataset on roads and settlements was obtained from the Department of Survey (<https://opendatanepal.com/dataset>), and the vector polyline and points shapefile were further rasterized using the Euclidean distance method under the spatial analyst tool. Table 1 provides information on the data model and the sources of the various criteria maps. All the variables used in the study are visualized in Figure 2.

**Table 1.** Datasets used and their sources

Variable type	Data	Format	Data period	Resolution	Sources/References
Dependent variable	Fire occurrence data	SHP	2001-2023	1,000 m	MODIS
Topographical	ASTER DEM	TIFF	2019	30 m	NASA/LAADS/DAAC/USGS (V003) (LP DAAC, 2019)
	Slope	TIFF	2019	30 m	
	Aspect	TIFF	2019	30 m	
Climatic	Land surface temperature	HDF	2001-2023	1,000 m	MODIS (Wan, 2014)
	Precipitation	TIFF	2000-2018	4.5 km	Worldclim
Bio-physical	Landcover (2010)	TIFF	2010	30 m	ICIMOD (ICIMOD, 2013)
Anthropogenic	Proximity of settlement	SHP	2015	1:25,000	Department of Survey
	Distance from road	SHP	2015	1:250,000	Department of Survey

## 2.3 Preparation of variables

Before running any model, it is imperative to statistically test the multicollinearity among the response variables as it may later impact the model estimation (Chang et al., 2013). In multiple regression models, multicollinearity refers to the level of linear intercorrelation between the explanatory variables (Kim, 2019). So, before relying on the input variable's authenticity, a multicollinearity test was conducted to observe the correlation among the independent variables in response to the dependent fire count, to accurately validate the data and obtain a reliable

conclusion. All the independent explanatory variables were classified as categorical variables before running the multicollinearity test. We calculated the Variation Inflation Factor (VIF) among the variables since it shows the severity of collinearity among the variables. The study of Davis et al. (2017) states that the variables with  $\text{VIF} < 5$  have insignificant levels of multicollinearity. As visible in Table 2, since the VIF for all the eight independent variables ranged below 1.6, thus indicating a low correlation between the input variables, all the variables were used for fire risk mapping.

As for the trend analysis of forest fire for the years 2001-2023, the Man-Kendall test was used for both the fire incidents and the burnt area. It assesses the significance of the Theil-Sen slope (Mann, 1945) and indicates the presence of a trend when the TS slope quantifies its magnitude. Different studies like

Mishra et al. (2014) and Zhu et al. (2023), have used it for forest fire and burnt area trend and significance estimation. Furthermore, to analyze the spatial distribution of forest fire counts across different variables, Arc GIS 10.8 (ESRI, 2022) was used to overlay the incidents and variables.

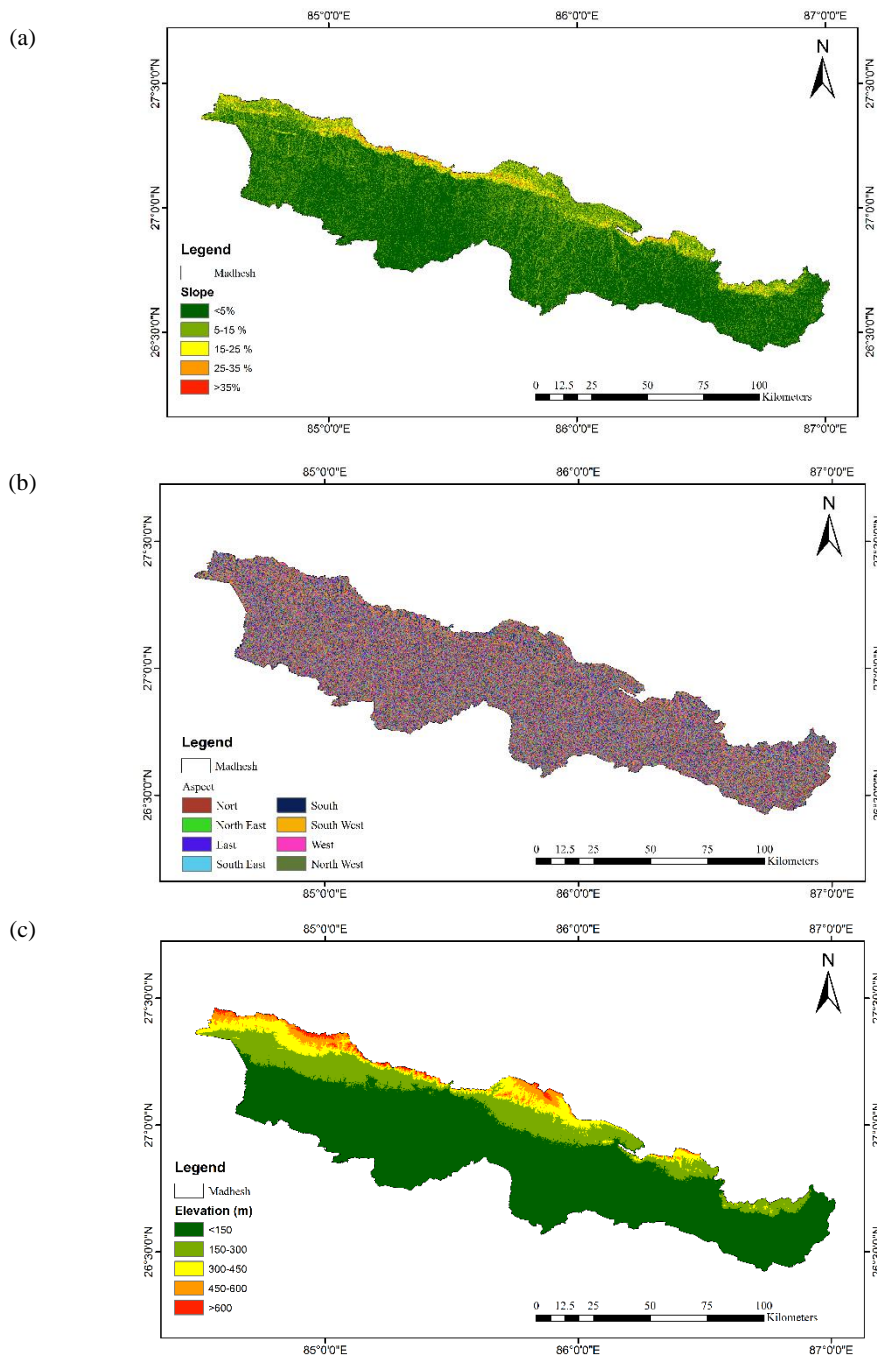


**Figure 2.** Variables (a) slope, (b) aspect, (c) elevation, (d) land surface temperature, (e) proximity of settlement, (f) distance from road, and (g) precipitation

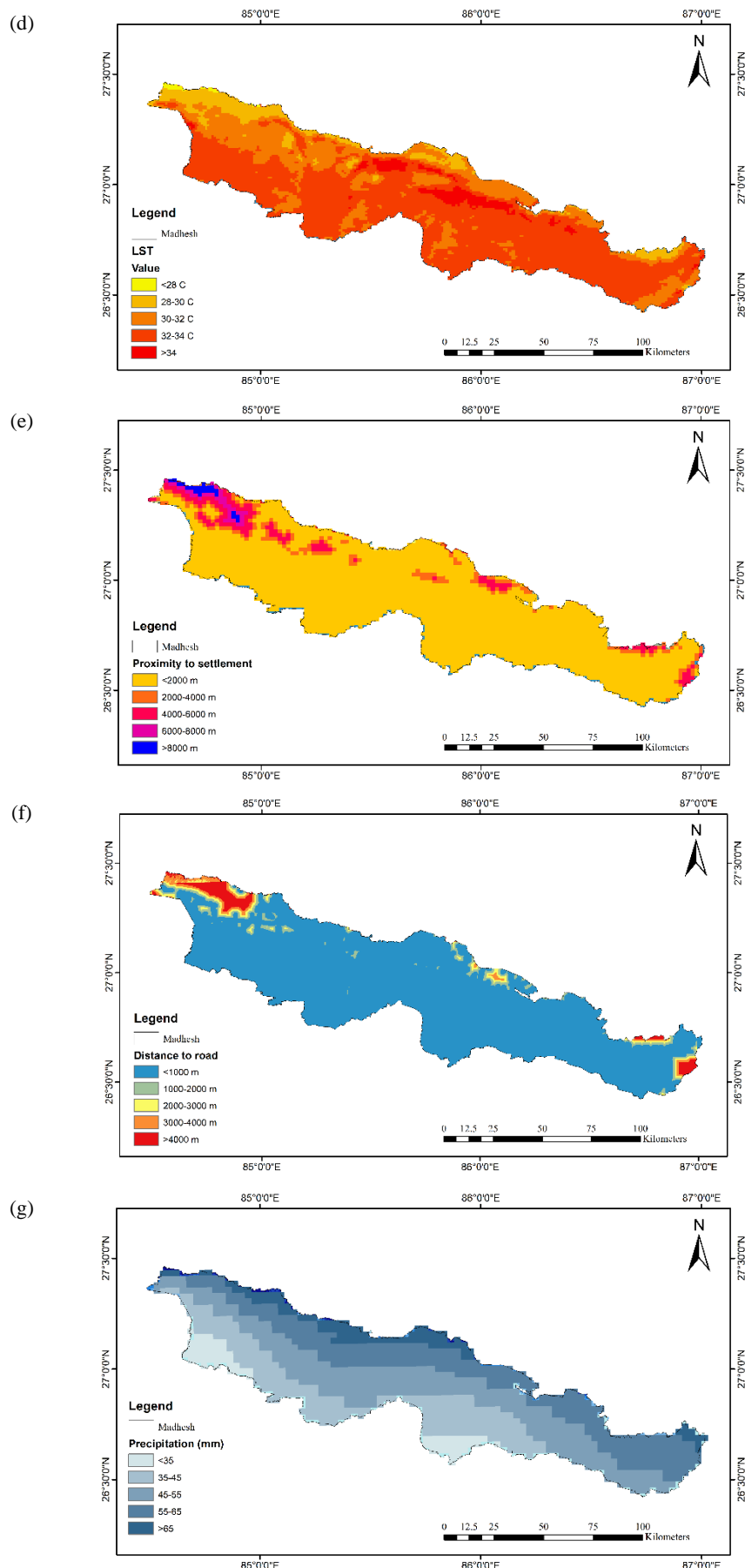


**Figure 2.** Variables (a) slope, (b) aspect, (c) elevation, (d) land surface temperature, (e) proximity of settlement, (f) distance from road, and (g) precipitation (cont.)

**Table 2.**VIF test of all the independent variables

Type of variable	Variable name	Collinearity statistics	
		Tolerance	VIF
Independent Explanatory Variables	Slope	0.968	1.033
	Settlement	0.728	1.374
	Road distance	0.656	1.524
	LST	0.650	1.538
	Elevation	0.999	1.001
	Land cover	0.808	1.237
	Aspect	0.999	1.001
	Precipitation	0.989	1.203

\*Dependent variable: Fire count

## 2.4 Assignment of weights for risk model

The weight ranking of each variable was done using the AHP method which is a pairwise comparison-based measurement theory and establishes the significance of each criterion (Saaty, 1994; Saaty, 1977; Saaty, 1988; Saaty and Vargas, 1991). Individual criteria and their subclasses are given relative weights based on previously acquired knowledge of the criteria's features, local field experience, firsthand observation, specifics of the chosen research area, and expert suggestions. A pairwise comparison matrix was made to compare all factors against each other based on their importance (equal, moderate, strong, very strong, and extremely strong). A standard Saaty's 1-9 scale was used to determine the relative importance values for all themes and their respective features, where value '1' denotes "equal importance" between the two themes, and the value '9' denotes the "extreme importance" of one theme compared to another as shown in [Table 3](#).

**Table 3.** Scale for a pair-wise comparison matrix (Saaty, 1988)

Intensity importance	Linguistic variables
1	Equal importance
2	Equal to moderate importance
3	Moderate importance
4	Moderate to strong importance
5	Strong importance
6	Strong to the very strong importance
7	Very strong importance
8	Very to the extremely strong importance
9	Extreme importance

Mathematical description of the different steps is summarized in the following steps.

(1) Sum the values in each column of the pairwise comparison matrix using the formula:

$$L_{ij} = \sum_{n=1}^n C_{ij} \quad (1)$$

Where;  $L_{ij}$  is the total column value of the pairwise comparison matrix and  $C_{ij}$  is the criteria used for the analysis.

(2) Divide each element in the matrix by its total row to generate a normalized pair-wise comparison matrix ([Table 5](#)) as shown in:

$$X_{ij} = \frac{C_{ij}}{L_{ij}} \quad (2)$$

Where;  $X_{ij}$ =normalized pair-wise comparison matrix.

(3) Divide the sum of the normalized row of the matrix by the number of criteria/parameter (N) to generate the standard weight by using the following formula:

$$W_{ij} = \frac{\sum_{j=1}^n X_{ij}}{N} \quad (3)$$

Where;  $W_{ij}$ =standard weight.

(4) For calculating the consistency vector values, the following formula was used:

$$\lambda = \sum_{n=1}^n C_{Vij} \quad (4)$$

Where;  $\lambda$ =consistency vector.

(5) Consistency index (CI) was used as a deviation or degree of consistency which was then calculated using the following Equation 5 and Consistency ratio (Cr) was calculated by using the formula Equation 6 ([Kanga et al., 2017; Kayet et al., 2018](#)).

$$CI = \frac{\lambda - n}{n-1} \quad (5)$$

Where; CI=consistency index, n=number of criteria.

(6) For calculating the Consistency ratio (Cr)

$$Cr = \frac{CI}{RI} \quad (6)$$

If the value of the Consistency ratio (Cr) is less than or equal to 0.10, then the inconsistency is acceptable (Barzilai, 1998). Random inconsistency (RI) values for 'n' number of criteria, i.e., the number of parameters are shown in Table 4.

**Table 4.** Random index (RI) for different number of criteria (n)

n	1	2	3	4	5	6	7	8	9	10
RI	0	0	0.58	0.9	1.12	1.24	1.32	1.41	1.45	1.49

**Table 5.** Pairwise and normalized comparison matrix

	LULC	PS	DR	Elevation	LST	Slope	Aspect	Rainfall	
LULC	1	3	3	5	5	6	7	7	
PS	0.33	1	3	4	5	5	6	7	
DR	0.33	0.33	1	3	3	4	5	5	
Elevation	0.2	0.25	0.33	1	3	3	5	6	
LST	0.2	0.2	0.33	0.33	1	2	3	7	
Slope	0.17	0.2	0.25	0.33	0.5	1	3	5	
Aspect	0.14	0.17	0.2	0.2	0.33	0.33	1	5	
Rainfall	0.14	0.14	0.2	0.17	0.14	0.2	0.2	1	
	LULC	PS	DR	Elevation	LST	Slope	Aspect	Rainfall	Total weight
LULC	0.4	0.57	0.36	0.36	0.28	0.28	0.23	0.16	2.64
PS	0.13	0.19	0.36	0.29	0.28	0.23	0.2	0.16	1.84
DR	0.13	0.06	0.12	0.21	0.17	0.19	0.17	0.12	1.17
Elevation	0.08	0.05	0.04	0.07	0.17	0.14	0.17	0.14	0.86
LST	0.08	0.04	0.04	0.02	0.06	0.09	0.1	0.16	0.59
Slope	0.07	0.04	0.03	0.02	0.03	0.05	0.1	0.12	0.46
Aspect	0.06	0.03	0.02	0.01	0.02	0.02	0.03	0.12	0.33
Rainfall	0.06	0.03	0.02	0.01	0.01	0.01	0.01	0.02	0.17
									Normal weight

Finally, the weight was assigned to the variables accordingly. The Cr value was calculated within the acceptable range of less than 0.01 (Barzilai, 1998). Relative weights were assigned to different classes of variables from local field experience, personal observation, previous research in similar regions, literature (Parajuli et al., 2020; Parajuli et al., 2023; Tiwari et al., 2021), and expert's suggestions. The expert group was constituted of four members including the expert personnel from the District Forest office, the Institute of Forestry, and the Ministry of

Tourism and Environment. Finally, the weight was assigned as shown in Table 6. For each variable, the classes for the impact of forest fire were classified into five different categories: Very High, high, medium, low, and very low based on the suggestions from experts, distribution of forest fire points (Figure 6), and different literature review (Parajuli et al., 2020; Parajuli et al., 2023; Tiwari et al., 2021). The methodological framework utilized in the study is given in Figure 3 which was used for obtaining the final risk map.

**Table 6.** Weight ranking for the different classes of the variables

Variable	Normalized weight	Class	Value assigned	Fire rating classes
Land cover	0.33	Broadleaved closed forest	1	Very high
		Broadleaved open forest	2	High
		Grassland	3	Medium
		Shrubland	4	Low

**Table 6.** Weight ranking for the different classes of the variables (cont.)

Variable	Normalized weight	Class	Value assigned	Fire rating classes
Land cover	0.33	Needle leaved open forest	4	Low
		Other	5	Very low
Slope (%)	0.06	<5	1	Very high
		5-15	2	High
		15-25	3	Medium
		25-35	4	Low
		>35	5	Very low
Distance to road (m)	0.15	<1,000	1	Very high
		1,000-2,000	2	High
		2,000-3,000	3	Medium
		3,000-4,000	4	Low
		4,000-5,000	5	Very low
Proximity to settlement (m)	0.22	<2,000	1	Very high
		2,000-4,000	2	High
		4,000-6,000	3	Medium
		6,000-8,000	4	Low
		>8,000	5	Very low
Elevation (m)	0.11	<150	1	Very high
		150-300	2	High
		300-450	3	Medium
		450-600	4	Low
		>600	5	Very low
LST	0.07	<28	5	Very low
		28-30	3	Medium
		30-32	2	High
		32-34	2	High
		>34	1	Very high
Aspect	0.04	South	1	Very high
		Southwest	1	Very high
		Southeast	2	High
		West	3	Medium
		East	3	Medium
		Northwest	4	Low
		Northeast	4	Low
		North	5	Very low
Precipitation (mm)	0.02	<35 mm	1	Very high
		35-45 mm	2	High
		45-55 mm	3	Medium
		55-65 mm	4	Low
		>65 mm	5	Very low

### 3. RESULTS AND DISCUSSION

#### 3.1 Trend analysis of fire incidents in Madhesh Province

From 2001 to 2023, altogether 6,796 fire incidents occurred across 6,158.22 km<sup>2</sup> in Madhesh Province. However, only the data with detection confidence greater than 30% accounted for 6,368 fire

incidents, as illustrated in [Figure 4](#). This study recorded the year 2021 with the highest fire incidents, while [Parajuli et al. \(2020\)](#) had regarded the year 2016 with the most fire incident occurrence, where [Parajuli et al. \(2023\)](#) has signified that both 2016 and 2021 witnessed severe drought conditions, pointing out as primary reason for sudden surge of fire incidents.

Previously, the research of [Parajuli et al. \(2015\)](#) and [Matin et al. \(2017\)](#) showed that the year 2009 had high

frequency of fire incidents due to persisting lower moisture regimes.

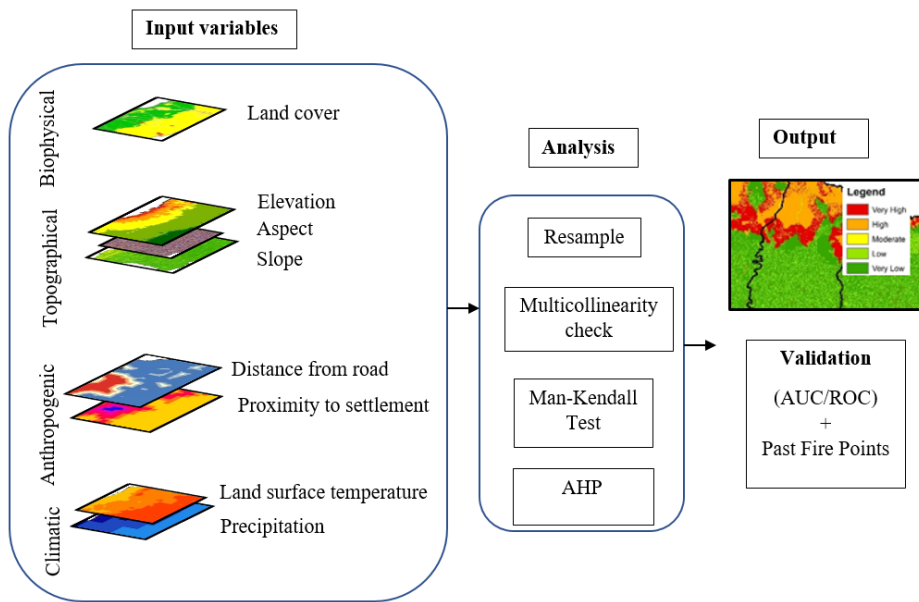


**Figure 3.** Methodological framework for forest fire risk map

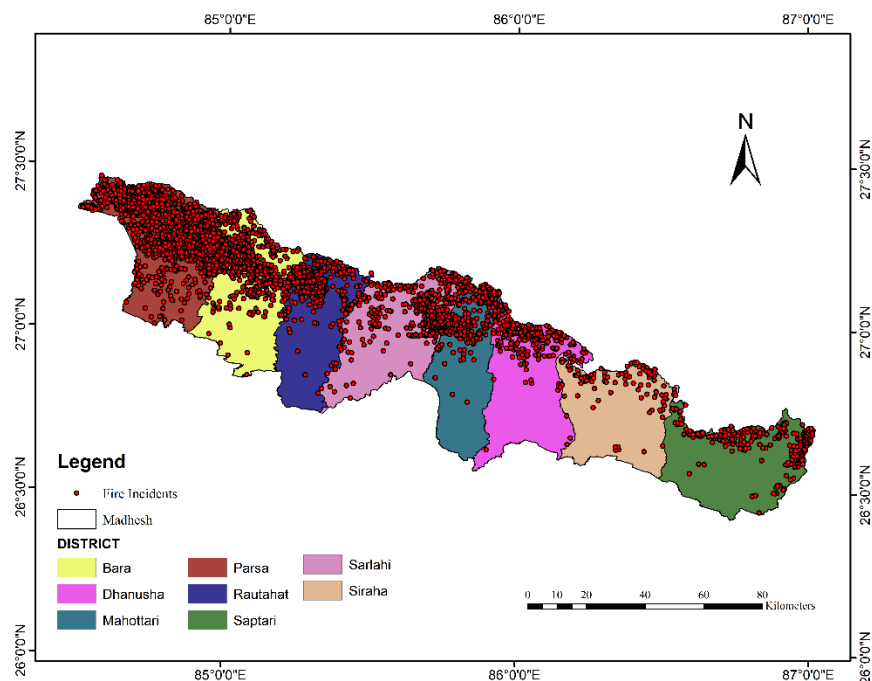


**Figure 4.** Fire incidents in Madhesh Province for the study period (2001-2023)

We used the Mann-Kendall trend analysis ([Mishra et al., 2014](#)) for burnt area analysis and it revealed a decreasing trend with Kendall's tau value of -0.11 and a Sen's slope value of -0.52 ([Figure 5\(a\)](#)). However, this decrease is of relatively low magnitude. Importantly, the observed negative trend in the burnt area is statistically insignificant ( $p=0.92$  at a 5% significance level). In [Figure 5\(b\)](#), the Mann-Kendall

trend analysis of fire incidents highlights a statistically significant trend ( $p=0.02$ ) of increasing forest fire incidence in the region. This is evidenced by the positive value of Kendall's tau (0.351) and Sen's slope value (10.5). The positive trend signifies a notable increase in forest fire incidents over the analyzed period.

Such phenomena may result from improved fire management and suppression efforts, which limit the spread of fires despite higher incident rates (Mishra et al., 2014). Additionally, factors like changes in land use and vegetation dynamics, as well as climatic variations, may play a role in causing

inconsistencies between burn area and fire incidence as seen in Figure 5 (Bowman et al., 2009; Westerling et al., 2006). These findings indicate a complex interplay of factors influencing fire dynamics, thus, requiring further investigation into the underlying causes of these trends.

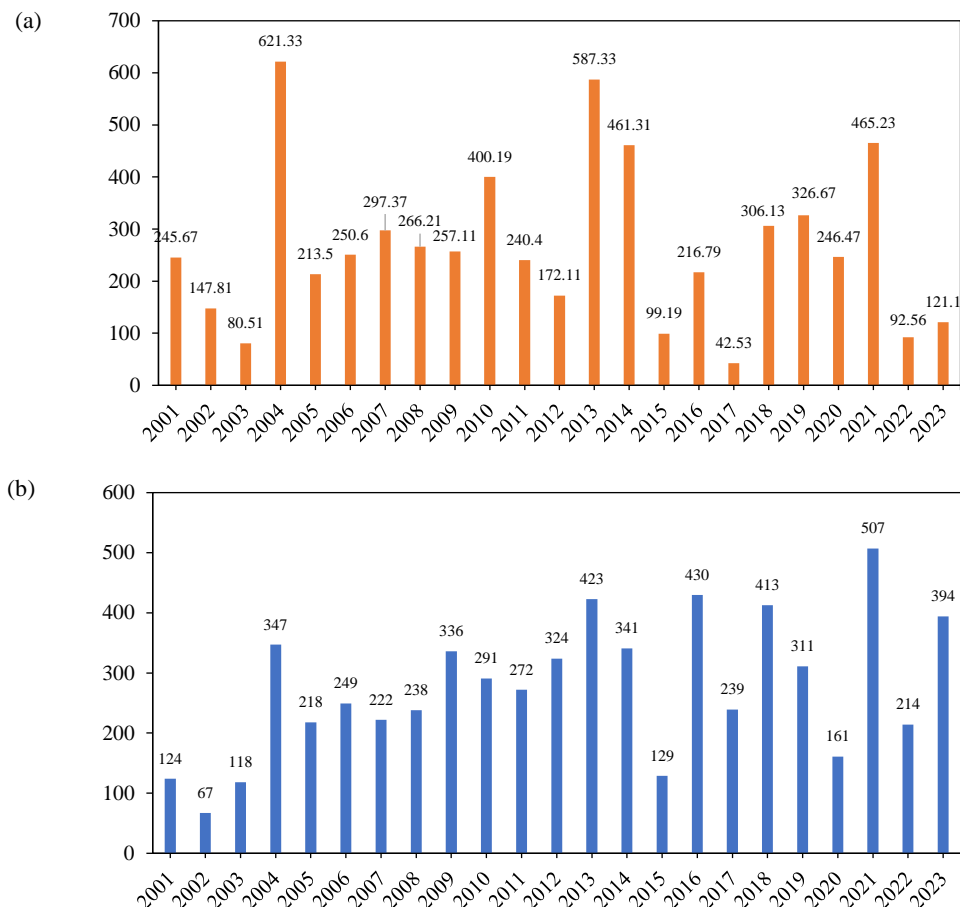


**Figure 5.** Year-wise trend analysis of forest fire in Madhesh Province: (a) Burnt area (per km<sup>2</sup>) and (b) Fire incidence reported by MODIS

### 3.2 Variables effect on forest fire incidents

Each factor concerned with forest fire has been discussed and analyzed separately. The land cover class map shows that around 16% of the study area was forested with broad-leaved closed forest comprising the majority area of approximately 83%. Figure 6(a) shows that the broad-leaved closed forest was intercepted with the highest number of forest fire counts consisting 74% of the total incidents. This was due to the presence of dried Sal (*Shorea robusta*) leaves serving as active fuel material, comprising almost 90% of the continuous fuel in the forest of this region (Sharma and Hussin, 1996).

The fire incidents witnessed a decreasing trend with the slope increment as shown in Figure 6(b). In case of plain lands, as of Terai Region of Nepal, the study of Matin et al. (2017) recorded that 72% of the

fires occurred in the areas with temperature above 30°C and a slope of less than 5%. Similar findings were recorded in this study where a majority of incidents occurred in the areas where temperature was around 30-32°C. Further, the southern side receives more sunshine, thus, raises the temperature and makes fuel drier (Prasad et al., 2008; Parajuli et al., 2020). Majority of the Madesh Province falls in the Terai Region with some extension in the Chure hills up to 918 m, fire incidents decreased with an increase in the elevation. As evident in Figure 6(c), only a quarter of fire incidents occurred in the areas with slope greater than 15%. Similar findings were reported by Ariapour and Shariff (2014), where 65% of fires occurred within 1,000 m elevation. Further, this study showed that the areas within the proximity of 2,000 m from settlements, there were relatively high fire incidents

comprising almost 45%. Interestingly, a slight increment from 1369 to 1428 is seen in fire incident occurrence between 2,000-6,000 m which later decreases to only about 14.5% incidents. According to research by [Hussin et al. \(2008\)](#), people seldom light fires at distances greater than 2000 m from where they live which may be the reason for lesser frequency of fire incidents above 2,000 m as shown in [Figure 6\(g\)](#). The study of [Ariapour and Shariff \(2014\)](#) documented 40% of fire incidents within 1 km from the road. Likewise, in this study, [Figure 6\(h\)](#) shows that around 65% of fire incidents were within 1 km from the road. The incidence of fire to activities such as throwing unlit cigarettes onto dry litter, and heating bitumen/asphalt for road surfacing are subjected to higher occurrences of forest fires within closer proximity of road ([Jaiswal et al., 2002](#); [Ariapour and Shariff, 2014](#)).

Various researchers have employed different variables and assigned varying degrees of importance. [Tiwari et al. \(2021\)](#), for instance, accorded the highest weight to elevation, whereas [Feizizadeh et al. \(2015\)](#) prioritized slope. Further, [Hassan et al. \(2020\)](#) emphasized rainfall and temperature. However, [Kodandapani et al. \(2008\)](#) acknowledged that forest type plays a pivotal role in fire occurrence and highlighted those broad-leaved forests are highly susceptible to fire during dry seasons. This research discovered that relatively higher impacts are constrained by land cover, followed by proximity to settlement, elevation, road distance, as shown by [Figure 6](#) and the risk map. We found that the risk areas mostly comprised forest areas with almost 90% of the forest area under high and very high-risk areas in the province ([Figure 7](#)).

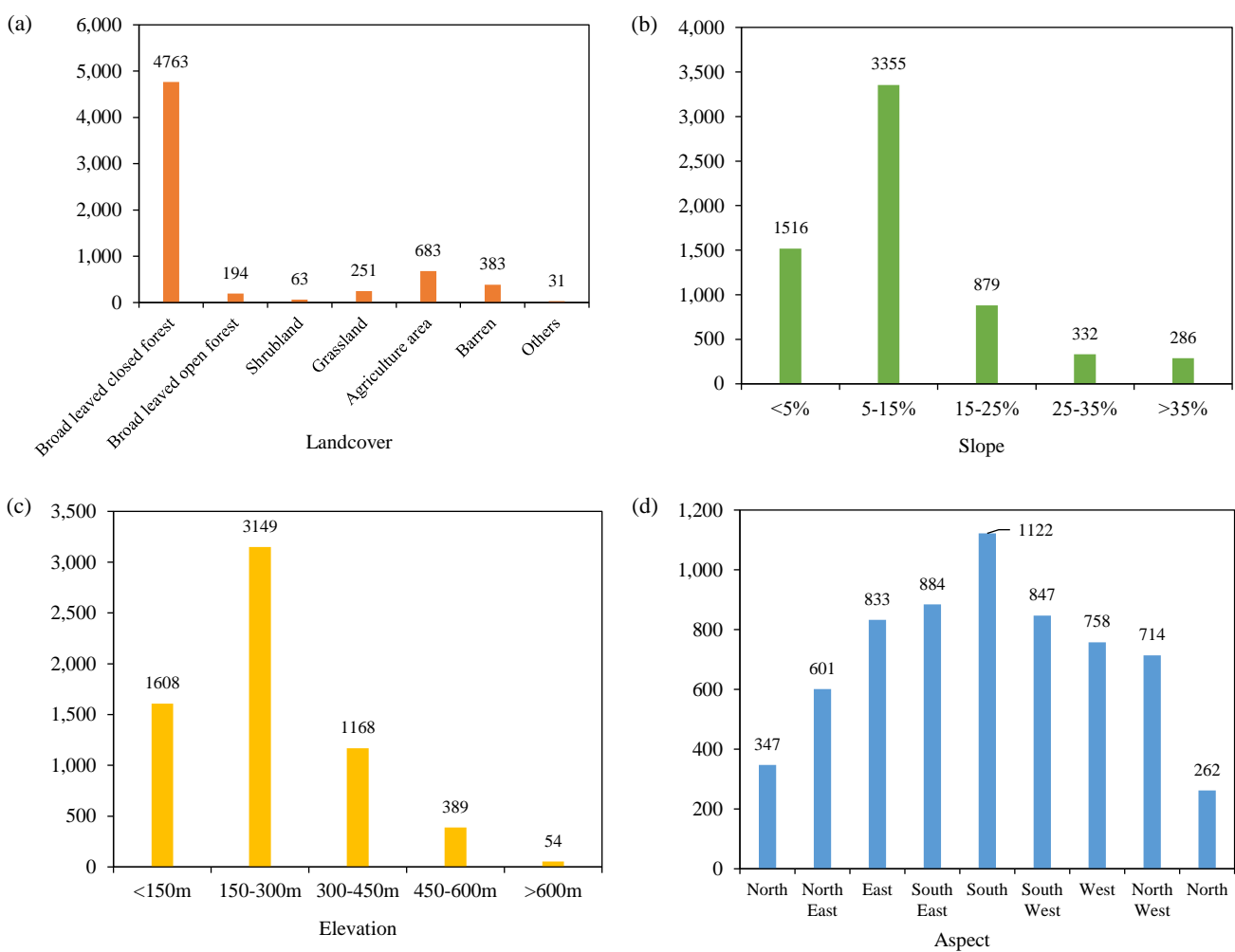


**Figure 6.** Forest fire incidents (a) land cover classes, (b) slope, (c) elevation, (d) aspect, (e) land surface temperature, (f) precipitation (g) proximity to settlement, and (h) distance to road

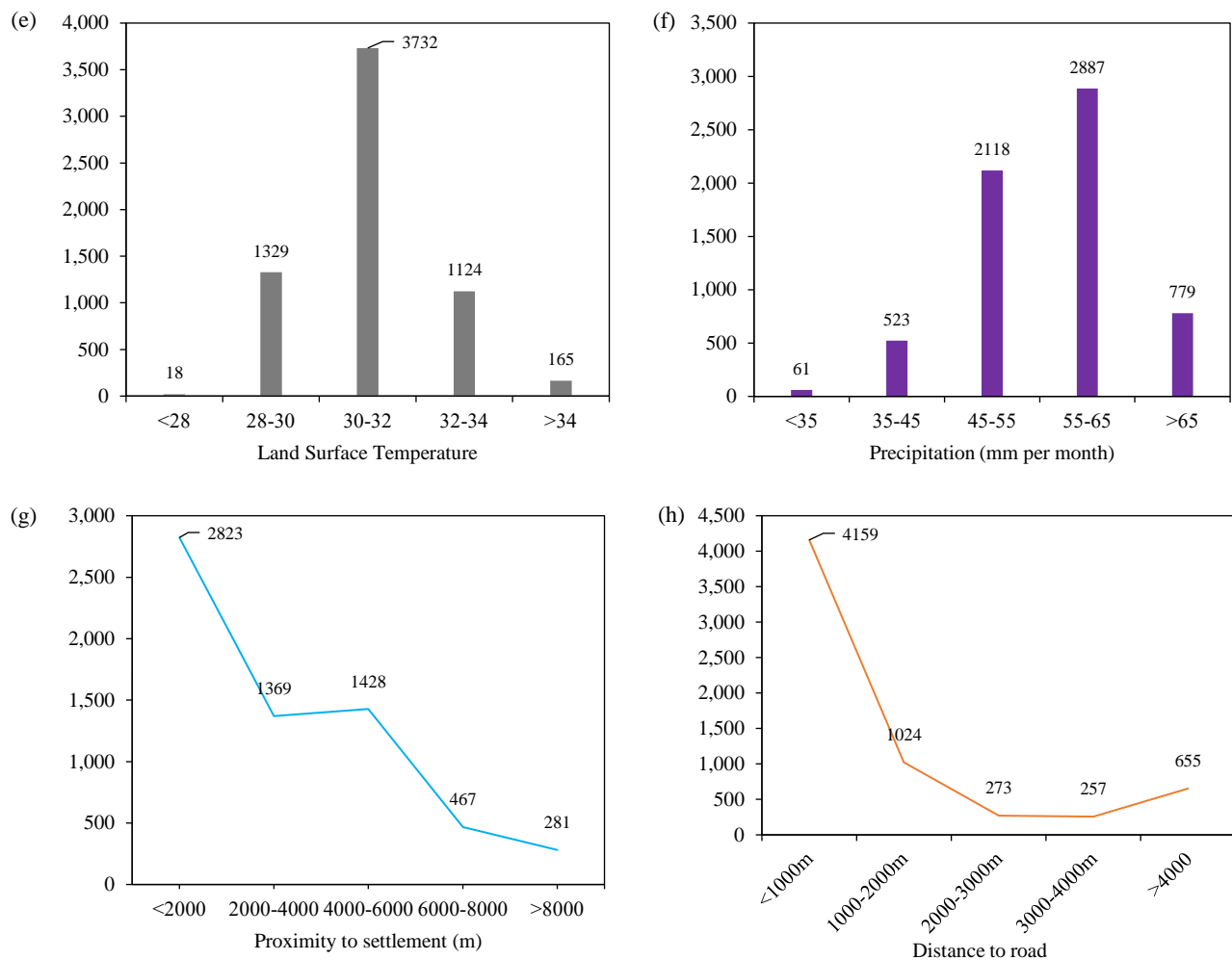


**Figure 6.** Forest fire incidents (a) land cover classes, (b) slope, (c) elevation, (d) aspect, (e) land surface temperature, (f) precipitation (g) proximity to settlement, and (h) distance to road (cont.)

### 3.3 Fire risk map

As accord to Table 6 weightage value obtained from the AHP method, the risk map of Madhesh was obtained. Based on the weightage given to each variable class as per their influence on forest fire, all the thematic variables were added using the weightage overlay method in ArcGIS as shown in Figure 7,

where the area is classified into five categories ranging from very high, high, moderate, and low to very low. The Table 7 demonstrates that, although the area under very high and high category is just 24.5%, however, it accounts for 72.5% of total fire incidents, which is in concordant with the output of Mann-Kendal trend analysis.

**Table 7.** Fire incidents in risk areas

Value	Area (km <sup>2</sup> )	% of area	No. of total fire counts	% of total fire counts	Fire density per km <sup>2</sup>
Very high	660.43	7.26	1,002	15.74	1.51
High	1566.52	17.24	3,679	56.78	2.34
Medium	193.36	2.13	556	8.73	2.87
Low	1430.45	15.72	558	8.76	0.39
Very low	5243.51	57.65	573	8.99	0.10

### 3.4 Validation

For the validation process, past data points were overlaid on the map, revealing a concentration of fire incidents in the high-risk zone. This validation method

aligns with approaches utilized by various researchers, including Higgins et al. (2013), Feizizadeh et al. (2015), Ajin et al. (2016), Pourghasemi (2020), and Lamat et al. (2021). Additionally, to ascertain the

accuracy of the results, the area under curve (AUC) curve was employed, as depicted in Figure 6. This study employed the AUC validation technique, like the approach utilized by Parajuli et al. (2023) and has yielded significant results. The ArcSDM tool (ESRI, 2022) was used in ArcGIS for AUC calculation and

the prediction map scored the AUC value of 0.798 (79.8%) (Figure 8) which shows the produced results are acceptable. Notably, this AUC value is comparable to that reported by (Tiwari et al., 2021) with 81.75% for AHP method.

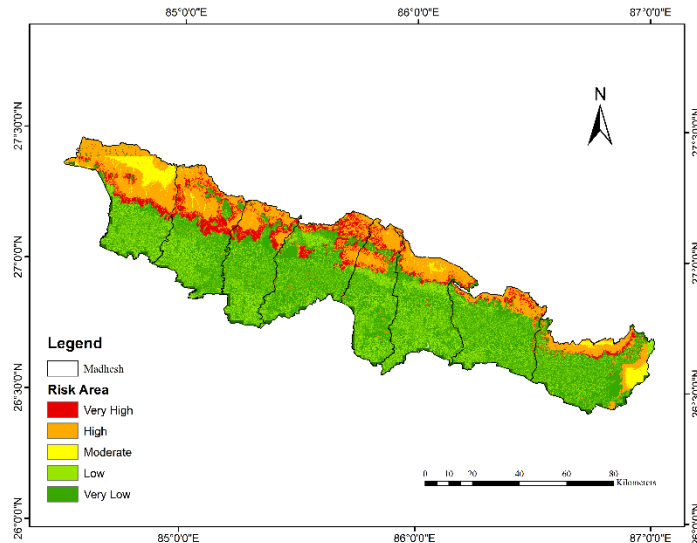


**Figure 7.** Forest fire risk map index combining all influencing variables

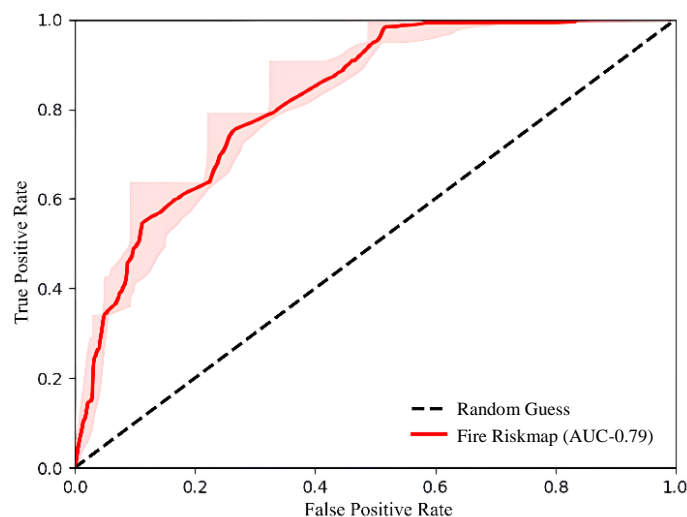


**Figure 8.** Receiver Operating Characteristic (ROC) curve of fire risk map

#### 4. CONCLUSION

The research gives insights to spatial dynamics of forest fires in various influencing variables in the sub-tropical forests of Madhesh Province of Nepal. The MODIS fire incidence analysis showed highest incidence in 2021 while highest burnt area was reported in 2004. Overall, the broadleaved forests appeared vulnerable to fire incidents occurrence, with nearly 90% of the forested area falling into high or very high-risk category, so mitigatory strategies are

suggested to be applied to lessen the damage incurred. The weight ranking shows that land cover, proximity to settlement, and elevation are highly sensitive to forest fire risk presumed in the Madhesh Province. Furthermore, the forest fire risk map index, based on the weightage of various variables, reveals that the forest area of the Madhesh Province is vulnerable, and overall, 7.26% area is under very high-risk, 17.24% under high risk. Moreover, the Man Kendall trend analysis of burn area and fire incidence reveal that

further intricated studies are required to understand the underlying factors affecting the variables associated with forest fires.

## ACKNOWLEDGEMENTS

This research acknowledges Department of Forest, Madhesh Province and Institute of Forestry Pokhara for providing necessary support and guidance throughout the research.

## AUTHOR CONTRIBUTIONS

- Conceptualization: Adhikari G and Joshi KP
- Data curation: Adhikari G;
- Formal analysis: Adhikari G and Joshi KP
- Funding acquisition: Not applicable
- Investigation: Adhikari G and Joshi KP
- Methodology: Adhikari G and Chad D
- Project administration: Not applicable
- Visualization: Adhikari G and Joshi KP
- Roles/Writing-original draft: Adhikari G, Mahara S, and Chad D
- Writing-review and editing: Mahara S, Adhikari G, and Ghimire A

## DECLARATION OF COMPETING INTEREST

The authors declare no conflict of interest.

## REFERENCES

- Ajin RS, Loghin AM, Vinod PG, Jacob MK. RS and GIS based forest fire risk zone mapping in the Periyar Tiger Reserve, Kerala, India. *Journal of Wetlands Biodiversity* 2016;6:139-48.
- Ariapour A, Shariff AR. Rangeland fire risk zonation using remote sensing and geographical information system technologies in Boroujerd Rangelands, Lorestan Province, Iran. *Ecopersia* 2014;2(4):805-18.
- Barzilai J. Consistency measures for pairwise comparison matrices. *Journal of Multi-Criteria Decision Analysis* 1998; 7(3):123-32.
- Bowman DM, Balch JK, Artaxo P, Bond WJ, Cochrane MA, D'Antonio CM, et al. Fire in the Earth system. *Science* 2009;324(5926):481-4.
- Chang Y, Zhu ZL, Bu RC, Chen HG, Feng YT, Li YH, et al. Predicting fire occurrence patterns with logistic regression in Heilongjiang Province. *Landscape Ecology* 2013;28(10): 1989-2004.
- Curkovic S. Sustainable development: Authoritative and leading edge content for environmental management. In: Leblon B, Chavez LB, Ayanz JSM, editors. *Use of Remote Sensing in Wildfire Management*. Croatia: InTech; 2012. p. 55-82.
- Davis R, Yang Z, Yost A, Belongie C, Cohen W. The normal fire environment-modeling environmental suitability for large forest wildfires using past, present, and future climate normals. *Forest Ecology and Management* 2017;390:173-86.
- Dawson TP, Butt N, Miller F. The ecology of forest fires. *ASEAN Biodiversity: The Newsmagazine of the ASEAN Regional Centre for Biodiversity Conservation* 2001;1(3):18-21.
- Department of Forest Research and Survey (DFRS). State of Nepal's Forests. *Forest Resource Assessment (FRA) Nepal*. Kathmandu, Nepal: DFRS; 2015.
- Doerr SH, Santín C. Global trends in wildfire and its impacts: Perceptions versus realities in a changing world. *Philosophical Transactions of the Royal Society B: Biological Sciences* 2016;371(1696):Article No. 20150345.
- Environmental Systems Research Institute (ESRI). *ArcGIS Desktop 10.8* [Internet]. 2022 [cited 2023 Mar 12]. Available from: <https://desktop.arcgis.com/en/arcmap/latest/get-started/installation-guide/installing-on-your-computer.htm>.
- Feizizadeh B, Omrani K, Aghdam FB. Fuzzy analytical hierarchical process and spatially explicit uncertainty analysis approach for multiple forest fire risk mapping. *Giforum* 2015;1:72-80.
- Giglio L, Schroeder W, Hall JV, Justice CO. *MODIS Collection 6 Active Fire Product User's Guide Revision A*. Maryland: Department of Geographical Sciences, University of Maryland; 2015. p. 9.
- Giglio L, Van der Werf GR, Randerson JT, Collatz GJ, Kasibhatla P. Global estimation of burned area using MODIS active fire observations. *Atmospheric Chemistry and Physics* 2006; 6(4):957-74.
- Food and Agriculture Organization of the United Nations (FAO). *Global Forest Resource Assessment* [Internet]. 2020 [cited 2023 Mar 12]. Available from: <http://www.fao.org/forest-resources-assessment/2020>.
- GoN/Ministry of Forests and Soil Conservation (MoFSC). *Conservation landscapes of Nepal*. Singha Durbar, Kathmandu, Nepal: Ministry of Forests and Soil Conservation; 2016.
- Hassan AH, Feizizadeh B, Blaschke T. GIS-based forest fire risk mapping using the analytical network process and fuzzy logic. *Journal of Environmental Planning and Management* 2020;63(3):481-99.
- Higgins E, Taylor M, Jones M, Lisboa P. Understanding community fire risk: A spatial model for targeting fire prevention activities. *Fire Safety Journal* 2013;62:20-9.
- Hussin YA, Matakala M, Zagdaa N. The applications of remote sensing and GIS in modeling forest fire hazard in Mongolia. *Proceedings of the 21<sup>st</sup> ISPRS Congress 2008: Silk Road for Information from Imagery*; 2008 July 3-11; Beijing: China; 2008.
- International Centre for Integrated Mountain Development (ICIMOD). *Land Cover of Nepal 2010*. ICIMOD; 2013.
- Jaiswal RK, Mukherjee S, Raju KD, Saxena R. Forest fire risk zone mapping from satellite imagery and GIS. *International Journal of Applied Earth Observation and Geoinformation* 2002;4(1):1-10.
- Joerin F, Thériault M, Musy A. Using GIS and outranking multicriteria analysis for land-use suitability assessment. *International Journal of Geographical Information Science* 2001;15(2):153-74.
- Kanga S, Tripathi G, Singh SK. Forest fire hazards vulnerability and risk assessment in Bhajji forest range of Himachal Pradesh (India): A geospatial approach. *Journal of Remote Sensing and GIS* 2017;8(1):1-6.
- Kayet N, Chakrabarty A, Pathak K, Sahoo S, Dutta T, Hatai B. Comparative analysis of multi-criteria probabilistic FR and AHP models for forest fire risk (FFR) mapping in Melghat Tiger Reserve (MTR) forest. *Journal of Forestry Research* 2018;31:565-79.

- Kim JH. Multicollinearity and misleading statistical results. *Korean Journal of Anesthesiology* 2019;72(6):558-69.
- Kodandapani N, Cochrane MA, Sukumar R. A comparative analysis of spatial, temporal, and ecological characteristics of forest fires in seasonally dry tropical ecosystems in the Western Ghats, India. *Forest Ecology and Management* 2008;256(4):607-17.
- Kumar D, Garg CP. Evaluating sustainable supply chain indicators using fuzzy AHP: Case of Indian automotive industry. *Benchmarking: An International Journal* 2017;24(6):1742-66.
- LP DAAC. ASTER Global Digital Elevation Model V003 [Internet]. 2019 [cited 2023 Mar 12]. Available from: <https://lpdaac.usgs.gov/products/astgtmv003/>.
- Lamat R, Kumar M, Kundu A, Lal D. Forest fire risk mapping using analytical hierarchy process (AHP) and earth observation datasets: A case study in the mountainous terrain of Northeast India. *SN Applied Sciences* 2021;3(4):Article No. 425.
- Mann HB. Nonparametric tests against trend. *Econometrica* 1945;13(3):245-59.
- Matin MA, Chitale VS, Murthy MSR, Uddin K, Bajracharya B, Pradhan S. Understanding forest fire patterns and risk in Nepal using remote sensing, geographic information system and historical fire data. *International Journal of Wildland Fire* 2017;26(4):276-86.
- Mishra B, Babel MS, Tripathi NK. Analysis of climatic variability and snow cover in the Kaligandaki River Basin, Himalaya, Nepal. *Theoretical and Applied Climatology* 2014;116: 681-94.
- Parajuli A, Chand DB, Rayamajhi B, Khanal R, Baral S, Malla Y. Spatial and temporal distribution of forest fires in Nepal. *Proceedings of the 14<sup>th</sup> World Forestry Congress*; 2015 Sep 7-11; Durban: South Africa; 2015.
- Parajuli A, Gautam AP, Sharma SP, Bhujel KB, Sharma G, Thapa PB, et al. Forest fire risk mapping using GIS and remote sensing in two major landscapes of Nepal. *Geomatics, Natural Hazards and Risk* 2020;11(1):2569-86.
- Parajuli A, Manzoor SA, Lukac M. Areas of the Terai Arc landscape in Nepal at risk of forest fire identified by fuzzy analytic hierarchy process. *Environmental Development* 2023;45:Article No. 100810.
- Pourghasemi HR, Kariminejad N, Amiri M, Edalat M, Zarafshar M, Blaschke T, et al. Assessing and mapping multi-hazard risk susceptibility using a machine learning technique. *Scientific Reports* 2020;10(1):Article No. 3203.
- Pradhan B, Suliman MDHB, Awang MAB. Forest fire susceptibility and risk mapping using remote sensing and geographical information systems (GIS). *Disaster Prevention and Management: An International Journal* 2007;16(3): 344-52.
- Prasad VK, Badarinath K, Eaturu A. Biophysical and anthropogenic controls of forest fires in the Deccan Plateau, India. *Journal of Environmental Management* 2008;86(1):1-13.
- Qadir A, Talukdar NR, Uddin MM, Ahmad F, Goparaju L. Predicting forest fire using multispectral satellite measurements in Nepal. *Remote Sensing Applications: Society and Environment* 2021;23:Article No. 100539.
- Ranabhat S, Pokhrel A, Neupane A, Singh B, Gahatraj S. Forest fire risk assessment and proposal for fire stations in different Geographical Regions of Central Nepal. *Journal of Forest and Livelihood* 2022;21(1):46-59.
- Reeves MC, Zhao M, Running SW. Applying improved estimates of MODIS productivity to characterize grassland vegetation dynamics. *Rangeland Ecology and Management* 2006; 59(1):1-10.
- Saaty TL. A scaling method for priorities in hierarchical structures. *Journal of Mathematical Psychology* 1977;15(3):234-81.
- Saaty TL. Some mathematical topics in the analytic hierarchy process. In: *Mathematical Models for Decision Support*. Berlin, Heidelberg: Springer; 1988.
- Saaty TL. How to make a decision: The analytic hierarchy process. *Interfaces* 1994;24(6):19-43.
- Saaty TL, Vargas LG. *Prediction, Projection and Forecasting*. Boston, USA: Kluwer Academic; 1991.
- Sharma N, Hussin Y A. *Spatial Modelling for Forest Fire Hazard Prediction, Management and Control in Corbett National Park, India*. University of Twente Research Information; 1996.
- Singh BK. Land tenure and conservation in Chure. *Journal of Forest and Livelihood* 2017;15(1):87-102.
- Tiwari A, Shoab M, Dixit A. GIS-based forest fire susceptibility modeling in Pauri Garhwal, India: A comparative assessment of frequency ratio, analytic hierarchy process and fuzzy modeling techniques. *Nat Hazards* 2021;105(2):1189-230.
- Wan Z. New refinements and validation of the collection-6 MODIS land-surface temperature/emissivity product. *Remote Sensing of Environment* 2014;140:36-45.
- Westerling AL, Hidalgo HG, Cayan DR, Swetnam TW. Warming and earlier spring increase western US forest wildfire activity. *Science* 2006;313(5789):940-3.
- Wang F, Hall GB, Subaryono. Fuzzy information representation and processing in conventional GIS software: Database design and application. *International Journal of Geographical Information System* 1990;4(3):261-83.
- Yu J, Chen Y, Wu J, Khan S. Cellular automata-based spatial multi-criteria land suitability simulation for irrigated agriculture. *International Journal of Geographical Information Science* 2011;25(1):131-48.
- Zolekar RB, Bhagat VS. Multi-criteria land suitability analysis for plantation in Upper Mula and Pravara basin: remote sensing and GIS approach. *Journal of Geographical Studies* 2018;2(1):12-20.
- Zhu H, Zhang Z, Yang S, Zhu ZP, Zeng AC, Guo FT. Temporal and spatial distribution of forest fire and the dynamics of fire danger period in southern and northern China: A case study in Heilongjiang and Jiangxi Provinces. *Chinese Journal of Ecology* 2023;42(1):Article No. 198-207.